

Smith

Shell Development Company

A Division of Shell Oil Company



Bellaire Research Center
P. O. Box 481
Houston, Texas 77001

3737 Bellaire Boulevard
Houston, Texas 77025

April 22, 1987

Mr. Dan Gibson
Amoco Production Company
Amoco Building
Denver, CO 80202

Mr. Terry Walden
Sohio Petroleum Company
2 Lincoln Centre
5420 LBJ Freeway
Suite 800/Lock Box 03
Dallas, TX 75240

Mr. Jim Poplin
Exxon Production Research Company
P. O. Box 2189
Houston, TX 77001

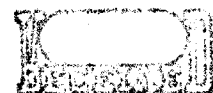
Mr. Charles Smith
U. S. Dept. of the Interior
Minerals Management Service
12203 Sunrise Valley Drive
Reston, VA 22091

Dear Participants:

MECHANICAL PROPERTIES OF SEA ICE - PHASE II (MPSI-2)

Enclosed is a draft copy of the paper entitled "Uniaxial and Biaxial Compressive Strength of Ice Sampled from Arctic Multiyear Pressure Ridges" by F. U. Hausler, E. N. Earle, and P. Gerchow. This paper is taken from the HSVA experimental study conducted as part of our MPSI-2 program and will be presented at POAC '87. The final report for the HSVA study was transmitted to you on January 24, 1984.

According to the Participation Agreement for MPSI, the confidentiality obligation for proprietary information extends for three years after the completion of a Phase. Although work on Phase II continued at CRREL well after the completion of the HSVA study, the CRREL work is an independent program and has no confidentiality restrictions. Consequently we view the January 1984 transmittal of the HSVA final report as satisfying the confidentiality obligation of the Participation Agreement. The Agreement also requires that publications resulting from any Phase acknowledge all participants who wish to be acknowledged. We

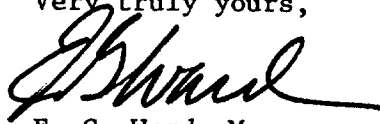


MPSI-2 Participants

2

will instruct the authors to acknowledge all MPSI-2 participants unless we are informed in writing by May 15, 1987 that a participant does not wish to be acknowledged.

Very truly yours,

A handwritten signature in dark ink, appearing to read 'E. G. Ward', written in a cursive style.

E. G. Ward, Manager
Offshore Engineering Research Department

Enclosure

AN/TO Fax No.: 001-713-663 2581
VON/FROM Fax No.: Hamburg 69 203 345

Datum/Date: March 23, 1987
Seitenzahl/No. of pages: 19

TELEFAX - MITTEILUNG / MESSAGE

AN/TO: Shell Development Company, Houston TX, U.S.A.
Offshore Engineering Research Department
z.Hd./Att.: Mr. E.G. Ward

VON/FROM: HAMBURGISCHE SCHIFFBAU-VERSUCHSANSTALT GmbH.
Bramfelder Straße 164, D-2000 Hamburg 60
Tel. No.: Hamburg / 6 92 03 - 0
Tlx. No.: 2 174 236 hsva d
F.U. Häusler 424
(6 92 03 - ...)



BETRIFFT/SUBJECT:

POAC-87 Paper on:
Uniaxial and biaxial compressive strength tests

TEXT:

Dear Mr. Ward:

Please find in the following the draft of the Shell-HSVA joint paper on the above topic. Please transfer a copy of it to Dr. E.N. Earle for approval. If there are any changes you or Dr. Earle recommend, please let us know as soon as possible. The deadline for draft manuscript is April 2, 1987.

Thank you in advance for your cooperation.

Yours sincerely

Franz Ulrich Häusler

Franz Ulrich Häusler

Uniaxial and biaxial compressive strength of ice sampled from Arctic multiyear pressure ridges

by F.U. Häusler

E.N. Earle

P. Gerchow

Hamburgische Schiffbau-Versuchsanstalt GmbH.

(formerly) Shell Development Company

Hamburgische Schiffbau-Versuchsanstalt GmbH.

A series of 60 compressive strength tests has been performed on ice sampled from multiyear pressure ridges near to Reindeer Is., Beaufort Sea. Three compressive stress states have been investigated: uniaxial ($\sigma_y = 0$) and biaxial with $\sigma_y = \sigma_x$ and $\sigma_y = 0.5 \sigma_x$.

Two temperature - strain rate combinations have been studied:
 $T_I = -5^\circ\text{C}$, $\dot{\epsilon}_x = 10^{-5} \text{s}^{-1}$ and $T_I = -20^\circ\text{C}$, $\dot{\epsilon}_x = 10^{-3} \text{s}^{-1}$.

For both T - $\dot{\epsilon}$ -combinations the coefficients of an isotropic 3-parameter yield criterion were evaluated representing the yield characteristics in the compression octant of the principal stress space. The multiyear pressure ridge ice was considered to behave isotropic on a macroscopic scale.

At $T_I = -20^\circ\text{C}$, $\dot{\epsilon}_x = 10^{-3} \text{s}^{-1}$ the ice exhibited brittle fracture. Under these conditions the measured compressive strengths were 5 times (uniaxial) up to 5.8 times (biaxial $\sigma_x = \sigma_y$) higher than at $T_I = -5^\circ\text{C}$, $\dot{\epsilon}_x = 10^{-5} \text{s}^{-1}$, where a mostly ductile mode of failure was observed.

The multiyear pressure ridge ice studied exhibited a wide variety of ice types (snow ice, columnar sea ice etc.). Ice densities were found from $\rho_I = 809 \text{ kg m}^{-3}$ up to 913 kg m^{-3} . The salinity measured in the samples' melts ranged from $S_I = 0$ up to 5.7 ‰ .

Introduction

The Alaskan and Canadian Arctic has proven to be one of the world's most important resources of hydrocarbons. Off-shore oil and gas exploration and exploitation in this region is impeded by ice of seasonally varying severity. In order to achieve a long (at best year round) drilling season, and at the same time to prevent ships and structures from damage or loss, both ships and structures must be designed to withstand ice loads. Another important aspect of safe operation is to preserve the sensitive Arctic environment from avoidable pollution.

One of the most hazardous forms of ice loads is exerted by multi-year pressure ridges which are by all means a common natural event in this region. Besides the driving forces (current, wind) and the response characteristics of the individual structure, the failure of multi-year ridge ice yields an important limiting condition for the ice loads. This condition may govern the structural design.

Multi-year pressure ridges can be defined as thick accumulations of broken ice blocks that have survived at least one melt season. The voids originally contained in the ridge from the pile up process are filled with refrozen water from surface melting. Thus a multi-year pressure ridge represents a huge piece of massive, nearly voidless ice. Its thickness may exceed 30 m (Kovacs, 1976 and 1983; Cox et al., 1984).

Information on the mechanical properties of multi-year ridge ice is scarce in literature, except the data reported by Kovacs (1983) and the results of the investigations by Cox et al. (1984 and 1985). The latter also contain the only strength data available up to now for multi-axial load conditions: compressive strengths under various lateral confinements.

In the present study, plane stress failure characteristics of multi-year ridge ice have been evaluated. For this purpose strength tests have been conducted under uniaxial compression and under biaxial compression with two different load ratios (1:1 and 2:1). The influence

of strain rate and temperature was investigated by performing the test at two different temperature strain rate combinations.

Ice field sampling and shipping

The field sampling was performed by CRREL personnel between 3 and 15 April 1981 in an area northwest of Reindeer Island in the Prudhoe Bay, Alaska (see Fig. 1). It was the same field campaign during which the samples were collected for Phase I of the comprehensive CRREL study on the mechanical properties of multi-year sea ice reported by Cox et al. (1984). Their report gives detailed descriptions of the sampling and shipping procedures, such that here only a short summary seems necessary.

The samples were collected from 10 multi-year ridges of various size. The ridges were part of the fast ice belt and were apparently not grounded. All ridges showed rounded outlines indicating surface melt processes in their history.

From each ridge, four vertical cores were drilled using a 108 mm (4.25 in.) fiberglass coring auger (Rand and Mellor, 1985). The cores were drilled in pairs (A-B and C-D) on two sites of each ridge. Depending on the ridge's size the sites were from 14 up to 46 m apart. Immediately after removal from the ice, the cores were catalogued and packed in core tubes. The tubes were then placed in insulated shipping boxes. In the field no measures have been taken for sample refrigeration, because the ambient air temperature of below -15°C was close enough to the $\text{NaCl}\cdot 2\text{H}_2\text{O}$ eutectic, -22.9°C , and because the multi-year ice had a low salinity (usually 4‰). The ice was then shipped by airfreight to CRREL, Hanover, N.H. where it was stored at -30°C (Cox, et al. 1984). On 25/26 October 1982 a lot of 10 tubes with ice samples was shipped to Hamburg again by airfreight. During all airfreight shipping the ice was refrigerated by dry ice. In Hamburg the ice core tubes were unpacked from the insulated boxes and stored in a freezing box at -35°C until test sample processing.

Test facilities

The strength test program was carried out on a triaxial closed-loop testing machine (Fig. 2). The vertical axis of this device consists of a screw driven universal testing machine of 100 kN load capacity type Schenk-Trebel RME 100. The two horizontal axes are provided by an HSVA-designed biaxial testing device with servo-hydraulic actuators of more than 100 kN load capacity each. The biaxial frame is mounted on the same base-frame as the RME 100. Thus the three axes form a monolithic unit. Each of the three axes is individually electronically closed-loop controlled. Coupling between the axes is performed electronically. For load application the testing machine is equipped with three pairs of brushlike loading platens (Hiledorf, 1965) especially designed for ice compression tests (Häusler, 1982). These loading platens consist of a cluster of slender metal rods (bristles) arranged in a quadratic array. They exhibit a high rigidity in the load direction combined with a minimal lateral constraint. Their transverse compliance allows the platens to follow lateral deformation of the tested specimen. Thus even true triaxial tests are possible. At least the edges of the samples always remain accessible to strain measuring devices (Linse, 1975; Häusler, 1982 and 1986). The complete loading apparatus is installed in a cold chamber where any temperature between -12 and -30 °C can be set. Electronic control and data acquisition devices are installed outside the cold room. For sample preparation a second cold room with an independent refrigeration system of the same capacity was used. It was equipped with a band saw and a lathe modified for milling cubic ice samples.

Fig 2?

Data acquisition and recording

Loads were measured by means of HBM (Hottinger Baldwin) Z4 200 kN load cells. For deformation measurements HBM W2K LVDTs were applied which have a maximum range of ± 2 mm. The primary axis' deformation transducer was installed in a parallelogram guide (see. Fig. 3). while the other LVDTs were mounted on pairs of bristles on the loading platen sides. Since the bristles follow the samples deformation, they can be used as

Fig 3?

pick up devices for deformation measurements.

The analogous signals from the transducers were on-line converted to digital on an HP 21 MXE series computer (Hewlett Packard) and stored on floppy discs for later off-line data processing. The digitizing rate was limited by the transfer rate from the AD-converter to the disc and by the storage capacity of the floppy disc. In the present study rates of 100 c.p.s. and 50 c.p.s. were applied in the high strain rate tests and of 4 c.p.s. in the low strain rate tests.

All other data such as temperatures or sample dimensions were recorded manually.

Sample preparation and test procedure

Sample preparation was done by cutting cubes of 69.8 ± 0.1 mm side length from the ice cores. This was done by first cutting the cores in cylindrical pieces of 10 cm length, and then cutting these pieces in raw cubes of about 8 cm side length. This was performed on a band saw. Fig. 4 shows the orientation of an ice cube in the parental core. The raw ice cubes were then milled down to their target dimensions on a modified lathe. For sample dimension control, a high precision stage with a dial gauge of 0.01 mm resolution was employed. In order to minimize brine drainage, sample preparation was performed at a temperature of about -25°C , i.e., below the $\text{NaCl} \cdot 2\text{H}_2\text{O}$ eutectic -22.9°C in sea ice.

The samples were then stored for one day at their target test temperature in order to achieve a homogenous temperature distribution within the samples when tested.

The work-off order of succession of the potential samples within the whole entity to be investigated was determined by drawing lots. By this means, a random distribution was achieved in the parameters not varied systematically, such as e.g., sampling site (core number), vertical position of a sample in its parental core or salinity.

Prior to each individual test, the sample's dimensions were measured again

and its weight was determined. Then the ambient air temperature and the ice temperature were recorded. The ice temperature was determined inside a reference ice cube of the same dimensions, which had undergone the same temperature history as the sample to be strength tested.

In the next step, the sample was installed in the loading device. The primary control axis' actuator was driven to a compressive preload of about $F \approx 0.25$ kN (corresponding stress 0.05 MPa), and kept these under static force control.

In the biaxial tests, the same was done with the secondary axis but with a preload corresponding to the target ~~load~~ load ratio. The secondary axis was then set to dynamic force control using the primary axis' force signal as a dynamic setting means. From here, the load ratio between the two axes was kept constant.

In the consequent steps of the procedure, the tips of the bristles used for strain measurements were frozen to the sample by a drop of water. Then the parallelogram guided deformation transducer, to be employed as actual value transducer for strain control, was put on top of the specimen parallel to the primary axis. Its tips were attached to two opposite bristles, such that deformation was measured between the loading platens. This allowed the continuation of a test even past sample fracture. The primary axis was then switched to closed-loop strain control.

During the test, the primary axis' strain was controlled by a dynamic setting means such that the ~~strain~~ strain-rate was constant. Test stop condition was the attainment of the target ~~strain~~ strain.

primary

primary

After the test, the sample or its debris was melted for salinity determination.

Data analysis

For each sampling cycle, the measured forces were converted into stresses using the equation

$$\sigma_i = F_i / A_i \quad (i = 1, 2) \quad (1)$$

with σ_i the stress and F_i the load in i -direction, and A_i the initial cross sec-

tion area normal to the i -direction.

Simultaneously, the deformations u in i -direction were transformed into strains ϵ_i using the simplified equation

$$\epsilon_i = u_i / C_i \quad (i = 1, 2, 3) \quad (2)$$

with C_i the initial distance between the pick-up points of the u_i -deformation transducer (basis length).

The initial tangent modulus was read from the slope of the σ_1 over ϵ_1 plots.

Because of the irregular distribution of ice types and crystal orientations within the ridge ice mass, the ice was assumed to behave isotropic on macro scale. Upon this assumption the ice failure condition can be described by the isotropic three-parameter yield function (Smith, 1974; Reinicke, 1977)

$$f(\sigma_{ij}) = \alpha J_1 + \beta J_2' + \gamma J_1^2 - 1 = 0 \quad (3)$$

where σ_{ij} is the stress tensor and J_1 its first invariant, while J_2' is the second invariant of the stress deviator s_{ij}

$$s_{ij} = \sigma_{ij} - \frac{1}{3} \delta_{ij} \sigma_{kk} \quad (4.1)$$

$$J_1 = \sigma_{kk} \quad (4.2)$$

$$J_2' = \frac{1}{2} s_{ij} s_{ij} \quad (4.3)$$

For a given temperature-strain rate condition the average strength values for the 3 different plane stress load conditions were computed. These averaged failure stress states were then used to determine the coefficients of the yield function

(5)

$$f(\sigma_{ij}) = a(\sigma_{11} + \sigma_{22}) + b(\sigma_{11}^2 + \sigma_{22}^2) + c\sigma_{11}\sigma_{22} - 1$$

which is the plane stress case of the three parameter yield function (eq. 3).

Results

The averaged test conditions: temperature, strain rate, density, and salinity are compiled in Table 1.

The average strengths (stresses at yield or failure) and initial tangent moduli are listed in Table 2.

The following characteristics have been

observed for the six test series:

Series 1000 ($\sigma_1:\sigma_2=1:1$, $T_I=-5^\circ\text{C}$, $\dot{\epsilon}_1=10^{-5}\text{s}^{-1}$)

The stresses' time histories exhibited a sharp rise until about half the yield stress. The yield stress was reached after a period of strain hardening at strains ϵ_1^y usually less than 1%. After yield, the stresses decreased slightly. At strains around 4% stresses increased again and reached or slightly exceeded the initial yield level. During some test runs, a reasonable amount of brine was squeezed out of the specimen, and formed icicles at the unloaded bottom surface. Cracks, if any, were of minor size and were in plane with the loads applied (Fig. 5; #1012).

Series 2000 ($\sigma_1:\sigma_2=2:1$, $T_I=-5^\circ\text{C}$, $\dot{\epsilon}_1=10^{-5}\text{s}^{-1}$)

The typical stress time history showed, as in series 1000, a sharp rise up to approximately half the yield stress followed by a period of strain hardening. Yield was reached at strains ϵ_1^y of usually less than 1%. Typically the stress decreased continuously after yield but apparently tended towards an asymptotic value to be encountered beyond the end of the tests ($\epsilon_1 > 5\%$). Cracks were of minor size and were in plane with the loads, similar to the pattern observed in series 1000.

Series 5000 ($\sigma_1:\sigma_2=1:0$, $T_I=-5^\circ\text{C}$, $\dot{\epsilon}_1=10^{-5}\text{s}^{-1}$)

The specimens exhibited an almost ductile mode of failure. In general no cracks have been observed. Deformation perpendicular to the load was large. Yield was reached at an average primary strain of $\epsilon_1^y = 0.7\%$.

Series 3000 ($\sigma_1:\sigma_2=1:1$, $T_I=-20^\circ\text{C}$, $\dot{\epsilon}_1=10^{-3}\text{s}^{-1}$)

The samples typically failed before having reached a zero slope in the stress over time (or strain respectively) curve. The failure mode was usually brittle. In some cases the first failure was not catastrophic but was followed by a second stress rise, which then was terminated by final failure. Only one single sample broke after a period of strain softening. The failure stress (first stress maximum) was typically reached at strains of $\epsilon_1^y = 0.25\%$. The samples were usually crushed during the

tests. The major surfaces of failure were slightly inclined to the plane expanded by the loads. In addition most of the samples were filled with microcracks (Fig. 6; #3013).

Series 4000 ($\sigma_1:\sigma_2=2:1$, $T_I=-20^\circ\text{C}$, $\dot{\epsilon}_1=10^{-3}\text{s}^{-1}$)

Typically, brittle failure was observed in the strain softening part of stress history. The average primary strain at yield was $\epsilon_1^y = 0.32\%$. The crack pattern was similar to the one observed in the series 3000 tests.

Series 6000 ($\sigma_1:\sigma_2=1:0$, $T_I=-20^\circ\text{C}$, $\dot{\epsilon}_1=10^{-3}\text{s}^{-1}$)

All samples failed more or less brittlely. After the tests, the samples were filled with cracks or totally crushed. In four (out of ten) cases, fracture occurred during or at the end of the stress rise. Fracture or yield was observed at an average primary strain of only $\epsilon_1 = 0.21\%$. The governing crack pattern exhibited crack surfaces oriented parallel to the load but without orientation in the two perpendicular directions. In some cases, parts of the samples failed in addition by buckling. The microcrack density was smaller than observed in the corresponding tests with biaxial load application (Series 3000 and 4000).

The plane stress yield functions (eq. 5) for the two temperature-strain rate combinations have been determined as follows

a) $T_I=-5.1^\circ\text{C}$, $\dot{\epsilon}_1=1.01 \cdot 10^{-5}\text{s}^{-1}$

$$f(\sigma_{ij}) = 1.78 \text{ MPa}^{-1} (\sigma_{11} + \sigma_{22}) + 1.78 \text{ MPa}^{-2} (\sigma_{11}^2 + \sigma_{22}^2) - 1.83 \text{ MPa}^{-2} \sigma_{11} \sigma_{22} - 1 = 0$$

b) $T_I=-20.1^\circ\text{C}$, $\dot{\epsilon}_1=0.99 \cdot 10^{-3}\text{s}^{-1}$

$$f(\sigma_{ij}) = 0.0476 \text{ MPa}^{-1} (\sigma_{11} + \sigma_{22}) + 0.0262 \text{ MPa}^{-2} (\sigma_{11}^2 + \sigma_{22}^2) - 0.0396 \text{ MPa}^{-2} \sigma_{11} \sigma_{22} - 1 = 0$$

The strength results presented graphically in Figs. 7 and 8. The upper left halves show the individually measured strengths while in the lower right halves the average values and 99% confidence interval bars are presented. Also shown for comparison are the results obtained at CRREL for the same ice under uniaxial tension and compression parallel to the parental core axis (Cox

*more expanded
→ clearer to read*

et al. 1984 and 1985).

Discussion

A comparison of the data from the present study with the results obtained at CRREL for the same ice (Cox et al. 1984 and 1985) is evident.

The discrepancy between the uniaxial compressive strengths seems obvious. Cox et al. (1984) report values of -2.34 ± 1.08 MPa for the $-5^\circ\text{C}/10^{-5}\text{s}^{-1}$ condition and -9.63 ± 1.39 MPa for the $-20^\circ\text{C}/10^{-3}\text{s}^{-1}$ condition (this study -1.40 ± 0.26 MPa and -7.26 ± 2.03 MPa). The main reason for this difference is the fact that the assumed isotropy of multi-year ridge ice is not fulfilled. In their "Phase II" test series Cox et al. (1985) have performed a comparison between horizontal and vertical compressive strengths at a strain rate of 10^{-4}s^{-1} . The vertical was 1.31 times (-5°C) and 1.65 times (-20°C) as high as the horizontal strength. The values of Cox et al. (1984) used above for comparison were obtained from vertical tests (parallel to the core's axis) while the strengths of the present study represent horizontal results.

Approximate horizontal compressive strengths can be calculated by correcting the vertical strengths with the horizontal to vertical ratios obtained from the 10^{-4}s^{-1} test. This correction yields $\sigma_c = -1.79 \pm 0.83$ MPa for the $-5^\circ\text{C}/10^{-5}\text{s}^{-1}$ case and $\sigma_c = -5.84 \pm 0.84$ MPa for the $-20^\circ\text{C}/10^{-3}\text{s}^{-1}$ case respectively. These values are in reasonable agreement with the results of the present study.

The coefficients of the yield functions evaluated, strictly speaking, cannot represent more than the plane stress failure characteristics under compression. Extrapolation to plane-stresses including tension is theoretically possible, but is usually inappropriate due to different failure mechanisms under tension and under compression.

Concerning the initial tangent moduli, only the value 6.33 ± 2.40 GPa determined at -20°C and 10^{-3}s^{-1} is supported by the corresponding modulus 7.62 ± 1.19 GPa measured by Cox et al. (1984). The value 0.87 ± 0.49 GPa measured in the

*expanded for
better readability*

present study for the -5°C and 10^{-5}s condition appears to be too low and is assumed to be due to larger initial setting of the brush platens in this case.

Comparison of the failure strains show for the $-20^{\circ}\text{C}/10^{-3}\text{s}^{-1}$ case almost identical values: $0.19 \pm 0.04\%$ (Cox et al.) and 0.21 (this study). The larger difference in the $-5^{\circ}\text{C}/10^{-5}\text{s}^{-1}$ case of $0.38 \pm 0.17\%$ (Cox et al.) compared to 0.7% (this study) may again be explained by the larger initial setting of the of the brush platens.

The density and salinity values given in Table 1 fit well with the data reported by Cox et al. (1985): $\rho = 891 \pm 26 \text{ kg m}^{-3}$ and $S = 1.26 \pm 0.82$ (Phase I only).

Conclusions

The present study provides horizontal and ~~un~~-axial compressive strengths of multi-year pressure ridge ice. The uniaxial strengths exhibit good agreement with the corresponding results obtained by Cox et al. (1984) for the same ice. This is remarkable, since Cox et al. have used 254 mm (10 in.) long nearly cylindrical specimens of 101.6 mm (4 in.) diameter with bonded synthane end caps (Mellor et al., 1984), while in the present study, cubic samples of 68.9 mm side length and brushlike loading platens have been employed. The good agreement achieved in spite of different testing techniques supports the credibility of both data sets and allows their combination for subsequent analyses.

The combined data sets provide an ample picture of the mechanical properties of ridge ice under the conditions investigated. Nevertheless, as already recognized by Cox et al. (1985), the broad structural variations encountered in natural pressure ridges as well as the lack of knowledge on near to melting conditions demand additional research work.

Acknowledgements

This paper is a joint contribution of the Hamburg Ship Model Basin (HSVA) and Shell Development Company. The support of the U.S. Army Cold Regions Research

Differences between Cox, et al. and the present study may be due in part to differences in sample geometry and boundary conditions

uniaxial and biaxial

and Engineering Laboratory (CRREL), namely Mrs. J.A. Richter-Menge given in sample shipping is gratefully acknowledged. Thanks are also expressed to the members of the staff of the HSVA ice engineering department who contributed to the present study, in particular to Mr. W. Neper who was in charge of sample preparation and technical assistance during test performance.

References

- Cox, G.F.N. et al., "Mechanical properties of multi-year sea ice - Phase I: Test results", U.S. Army Cold Regions Research and Engineering Laboratory, Hanover, N.H. Report 84-9, April 1984.
- Cox, G.F.N. et al., "Mechanical properties of multi-year sea ice - Phase II: Test results". CRREL Report 85-16, October 1985.
- Häusler, F.U., "Multiaxial Compressive Strength Tests on Saline Ice with Brush-Type Loading Platens". IAHR Symposium on Ice; Proceedings, Vol. II, pp. 526-539, Québec, Canada, 1982.
- Häusler, F.U., "Multiaxial mechanical properties of urea doped ice". IAHR Symposium on Ice Proceedings, Vol. I, pp. 349-363, Iowa City, USA, 1986.
- Hilsdorf, H., "Bestimmung der zweiachsigen Festigkeit des Betons". Deutscher Ausschluß für Stahlbeton, Heft 173, Berlin 1965.
- Kovacs, A., "Grounded ice in the fast ice zone along the Beaufort Sea coast of Alaska". CRREL Report 76-32, September 1976.
- Kovacs, A., "Characteristics of multi-year pressure ridges". POAC Proceedings, Vol. 3, pp. 173-182, Helsinki, Finland, 1983.
- Linse, D., "Lösung versuchstechnischer Fragen bei der Ermittlung des Festigkeits- und Verformungsverhaltens von Beton unter dreiachsiger Beanspruchung mit ersten Versuchen". Technische Universität München, 1975.
- Mellor, M., Cox, G.F.N., Bosworth, H., "Mechanical properties of multi-year sea ice - Testing Techniques". CRREL Report 84-8, 1984.

Smith, M.B., "A parabolic yield condition for anisotropic rocks and soils". Ph.D. Thesis, Rice University, Houston, TX, USA, 1974.

Reinicke, K.M., "Plasticity Analysis with an Isotropic Three-Parametric Yield Function". Unpublished report. BEB Gewerkschaften Brigitta und Elwerath, Hannover, Germany, 1977.

Rand, J. and Mellor, M., "Ice-coring augers for shallow depth sampling". CRREL Report 85-21, 1985.

Photographs in b/w

MSVA
Report
Fig.

Figures

- | | | |
|-----|--------|--|
| new | Fig. 1 | Map of ice sampling area (after Cox et al., 1984) |
| 3,1 | Fig. 2 | Triaxial closed-loop testing machine |
| 6,4 | Fig. 3 | Deformation transducer with parallelogram guided LVDT attached to a pair of opposite bristles of the brushlike loading platens at the end of a biaxial test (Series 1000). |
| new | Fig. 4 | Orientation of a cubic sample in its parental core |
| 6,5 | Fig. 5 | Sample #1012 after biaxial compression test with $\sigma_1 = \sigma_2$, $\sigma_3 = 0$, at -5°C and 10^{-3}s |
| 6,9 | Fig. 6 | Sample #3013 after biaxial compression test with $\sigma_1 = \sigma_2$, $\sigma_3 = 0$ at -20°C and 10^{-3}s |
| new | Fig. 7 | Plane stress strengths of multi-year ridge ice at -5°C and 10^{-3}s |
| new | Fig. 8 | Plane stress strengths of multi-year ridge ice at -20°C and 10^{-3}s |

-2-

Series	Temperature T_I [°C]	Strain rate at yield ϵ_1 [s ⁻¹]	Stress ratio $\sigma_1 = \sigma_2$	Density ρ_I [kg m ⁻³]	Salinity S [‰]
1000	5.0 ± 0.1	1.00 ± 0.00·10 ⁻⁵	1:1	868 ± 36	1.8 ± 1.0
2000	-5.1 ± 0.1	1.00 ± 0.01·10 ⁻⁵	2:1	889 ± 15	1.3 ± 0.6
3000	-20.2 ± 0.1	1.00 ± 0.09·10 ⁻³	1:1	909 ± 4	1.3 ± 0.6
4000	-20.2 ± 0.1	0.98 ± 0.09·10 ⁻³	2:1	890 ± 23	1.9 ± 0.7
5000	-5.2 ± 0.1	1.01 ± 0.00·10 ⁻⁵	1:0	873 ± 31	1.7 ± 1.3
6000	-19.9 ± 0.1	0.99 ± 0.11·10 ⁻⁵	1:0	886 ± 17	2.5 ± 1.6
1000 2000 5000	-5.1 ± 0.1	1.01 ± 0.01·10 ⁻⁵	all	880 ± 27	1.6 ± 1.0
3000 4000 6000	-20.1 ± 0.2	0.99 ± 0.09·10 ⁻³	all	895 ± 19	1.9 ± 1.2

Table 1 Test conditions

Series	Primary stress at yield σ_1 [MPa]	Secondary stress at yield σ_2 [MPa]	Initial tangent modulus E [GPa]	Number of tests
1000	-2.30 ± 0.90	-2.30 ± 0.91	---	10
2000	-2.33 ± 0.23	-1.12 ± 0.11	---	10
3000	-13.37 ± 1.87	-13.32 ± 1.86	---	10
4000	-11.98 ± 2.12	-5.98 ± 1.04	---	10
5000	-1.40 ± 0.26	---	0.87 ± 0.49	10
6000	-7.16 ± 2.03	---	6.33 ± 2.40	10

Table 2 Average strengths and elastic properties

-hh-

Fig. 1

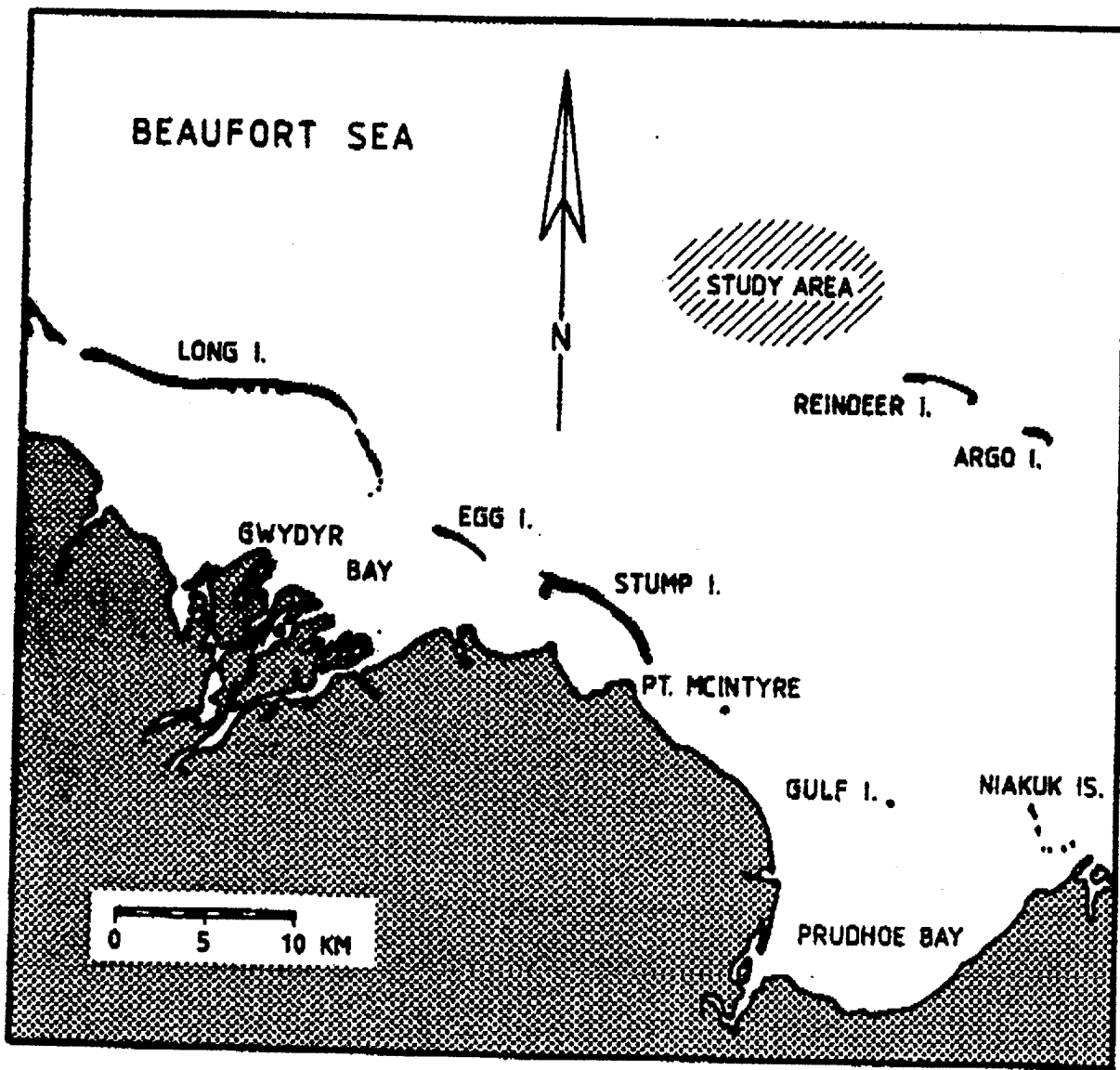


Fig. 2.1: Location of sample collection (map after Cox et al., 1982)

Fig. 4

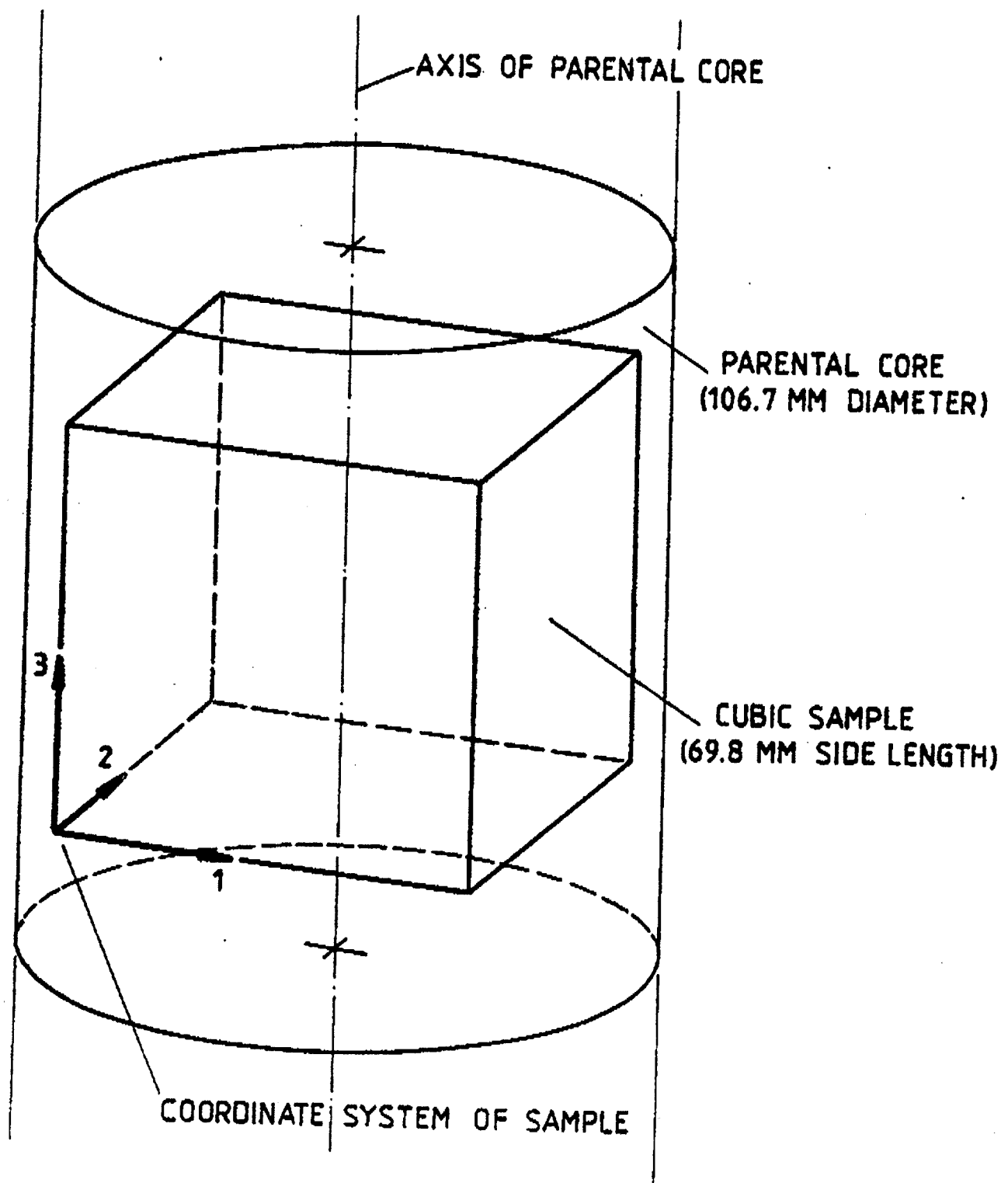


Fig. 7

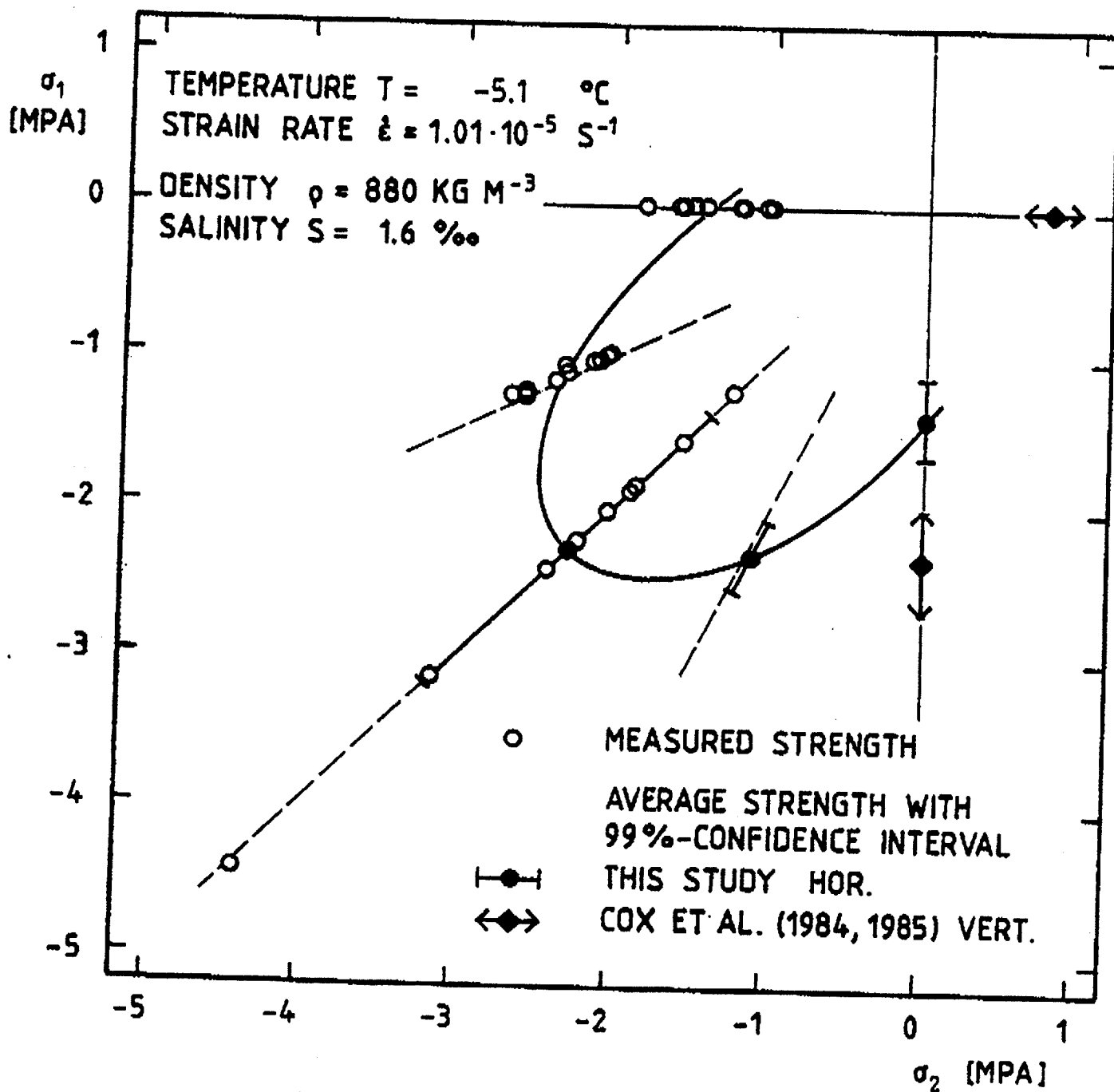


Fig. 8

- 13 -

